Powell William (Orcid ID: 0000-0002-8507-4038)

Novel highly potent OXE receptor antagonists with prolonged plasma lifetimes that are converted to active metabolites in vivo in monkeys

Running title: Potent OXE receptor antagonists with prolonged lifetimes

Qiuji Ye[1,†], Shishir Chourey[1,‡], Chintam Nagendra Reddy[1,§], Rui Wang[1], Chantal Cossette[2], Sylvie Gravel[2], Irina Slobodchikova[3], Dajana Vuckovic[3], Joshua Rokach[1], and William S. Powell[2]

[1]Claude Pepper Institute and Department of Chemistry, Florida Institute of Technology, 150 West University Boulevard, Melbourne, FL 32901-6982, USA

[2]Meakins-Christie Laboratories, Centre for Translational Biology, McGill University Health Centre, 1001 Decarie Blvd, Montreal, QC H4A 3J1, Canada

[3] Department of Chemistry and Biochemistry and PERFORM Centre, Concordia University, 7141 Sherbrooke St. W., Montréal, QC H4B 1R6, Canada

[†]Present address: Dept. Chemistry, Rice University, 6100 Main Street, Houston, TX 77005, USA

[‡]Present address: Chemical Development Dept., Albany Molecular Research Inc., 21 Corporate Circle, Albany, NY 12203, USA

[§]Present address: Olon Ricerca Bioscience, 7528 Auburn Road, Concord, OH 44077, USA

Word count: 4547 (Introduction: 941; Results: 2175; Discussion: 1431)

Abstract: 244 words

References: 37

This article has been accepted for publication and undergone full peer review but has not been through the copyediting, typesetting, pagination and proofreading process which may lead to differences between this version and the Version of Record. Please cite this article as doi: 10.1111/bph.14874

Acknowledgements

This work was supported by the Canadian Institutes of Health Research (WSP: Grants MOP-6254 and PP2-133388), the American Asthma Foundation (JR: Grant 12-0049), and the National Heart, Lung, and Blood Institute (JR: Grant R01HL081873) and by AmorChem (Montreal, QC). The Meakins-Christie Laboratories-MUHC-RI are supported in part by a Centre grant from Le Fond de la Recherche en Santé du Québec as well as by the J. T. Costello Memorial Research Fund. JR also wishes to acknowledge the National Science Foundation for the AMX-360 (Grant CHE-90-13145) and Bruker 400 MHz (Grant CHE-03-42251) NMR instruments. DV and IS were supported by the Natural Sciences and Engineering Research Council of Canada (Grant RGPIN/435814-2103). IS also wishes to acknowledge the Centre for Biological Applications of Mass Spectrometry at Concordia University for PhD scholarship funding. The content is solely the responsibility of the authors and does not necessarily represent the official views of the National Heart, Lung, and Blood Institute or the National Institutes of Health.

Author contributions

Q.Y., S.C., C.N.R. and R.W. performed the chemical syntheses. S.G. evaluated antagonist potencies. C.C. conducted HPLC analyses. I.S. and D.V. performed mass spectrometric analyses. W.S.P. and J.R. designed the study. W.S.P, J.R., Q.Y., S.C. and D.V. wrote or contributed to the writing of the manuscript.

Conflict of interest

W.S.P. and J.R. have been granted a patent covering **230** and have applied for a patent covering ***S*-Y048**.

Declaration of transparency and scientific rigour

This Declaration acknowledges that this paper adheres to the principles for transparent reporting and scientific rigour of preclinical research as stated in the *BJP* guidelines for Design & Analysis, and Animal Experimentation, and as recommended by funding agencies, publishers and other organisations engaged with supporting research.

Abstract

Background and Purpose: The 5-lipoxygenase product 5-oxo-6,8,11,14-eicosatetraenoic acid (5-oxo-ETE), acting through the OXE receptor, is a potent eosinophil chemoattractant that may be an important proinflammatory mediator in eosinophilic diseases such as asthma. We previously identified a series of indole-based OXE receptor antagonists that rapidly appear in the blood following oral administration but have limited lifetimes. The objective of this study was to increase the potency and plasma half-lives of these compounds and thereby identify the optimal candidate for future preclinical studies in monkeys, since rodents do not have an OXE receptor ortholog.

Experimental Approach: We synthesized a series of substituted phenylalkyl indoles and compared their antagonist potencies, pharmacokinetics, and metabolism to those of our earlier compounds. The potencies of some of their metabolites were also investigated.

Key Results: Among the compounds tested, the ***S***-enantiomer of the m-chlorophenyl compound (***S*-Y048**) was the most potent, with an pIC_{50} of about 10.8 for inhibition of 5-oxo-ETE-induced calcium mobilization in human neutrophils. When administered orally to cynomolgus monkeys, ***S*-Y048** rapidly appeared in the blood and had a half-life in plasma of over 7 h, considerably longer than any of the other OXE analogs tested. A major hydroxylated metabolite, with a potency close to that of its precursor, was identified in plasma.

Conclusion and Implications: Because of its highly potent antagonist activity and its long lifetime in vivo, ***S*-Y048** may be a useful anti-inflammatory agent for the treatment of eosinophilic diseases such as asthma, allergic rhinitis, and atopic dermatitis.

What is already known

- The eicosanoid 5-oxo-ETE is a potent eosinophil chemoattractant that acts via the OXE receptor.
- OXE receptor activation can be blocked by indole-based antagonists mimicking the structure of 5-oxo-ETE.

What this study adds

- We have structurally modified our OXE antagonists to substantially increase both potency and plasma half-life.

- ***S*-Y048** and its active hydroxylated metabolite have potencies in the picomolar range.

What is the clinical significance

- ***S*-Y048** is a good candidate for in vivo efficacy studies in monkeys.
- This OXE receptor antagonist may be a novel therapeutic agent in eosinophilic diseases in humans.

Abbreviations

230, 5-(5-chloro-2-hexyl-1-methyl-1*H*-indol-3-yl)-3-methyl-5-oxopentanoate
5-LO, 5-lipoxygenase
5-oxo-ETE, 5-oxo-6E,8Z,11Z,14Z-eicosatetraenoic acid
C025, 5-(5-chloro-1-methyl-2-(6-phenylhexyl)-1*H*-indol-3-yl)-3-methyl-5-oxopentanoic acid
***S*-C025**, (*S*)-5-(5-chloro-1-methyl-2-(6-phenylhexyl)-1*H*-indol-3-yl)-3-methyl-5-oxopentanoic acid
LT, leukotriene
MMP-9, matrix metalloproteinase-9
NP-HPLC, normal-phase-high performance liquid chromatography
RP-HPLC, reversed-phase-high performance liquid chromatography
***S*-230**, (*S*)-5-(5-chloro-2-hexyl-1-methyl-1*H*-indol-3-yl)-3-methyl-5-oxopentanoate
***S*-Y048**, (S)-5-(5-chloro-2-(6-(3-chlorophenyl)hexyl)-1-methyl-1H-indol-3-yl)-3-methyl-5-oxopentanoate
***S*-Y048M**, (S)-5-(5-chloro-2-((S)-6-(3-chlorophenyl)-1-hydroxyhexyl)-1-methyl-1H-indol-3-yl)-3-methyl-5-oxopentanoate
uPAR, urokinase-type plasminogen activator receptor
Y048, 5-(5-chloro-2-(6-(3-chlorophenyl)hexyl)-1-methyl-1H-indol-3-yl)-3-methyl-5-oxopentanoate.

Keywords: Lipid mediators; eicosanoids; 5-lipoxygenase products; 5-oxo-ETE; inflammation; asthma; GPCR antagonists

Introduction

Arachidonic acid metabolites formed by the 5-lipoxygenase (5-LO) pathway are important mediators in asthma and drugs targeting their biosynthesis reduce disease symptoms in

humans (Haeggstrom, 2018; Peters-Golden & Henderson, 2007). While the focus has principally been on leukotriene (LT) D_4, acting through the selective $cysLT_1$ receptor (Peters-Golden & Henderson, 2007; Yokomizo *et al.*, 2018), other 5-LO products may also play a role. LTB_4, LTD_4, and other cysLTs are only very weak chemoattractants for human eosinophils (Morita *et al.*, 1989; Powell *et al.*, 1995; Sun *et al.*, 1991), which play a major role in asthma and other allergic diseases (McBrien & Menzies-Gow, 2017). In contrast, another 5-LO product, 5-oxo-6,8,11,14-eicosatetraenoic acid (5-oxo-ETE), is a potent eosinophil chemoattractant, both in vitro (Powell *et al.*, 1995) and in vivo (Muro *et al.*, 2003). Its actions are mediated by the G protein-coupled oxoeicosanoid (OXE) receptor (Bäck *et al.*, 2014; Hosoi *et al.*, 2002; Jones *et al.*, 2003; Takeda *et al.*, 2002), which is encoded by the *OXER1* gene. The OXE receptor is highly expressed on eosinophils and basophils and to a lesser extent on neutrophils, monocytes and macrophages (Iikura *et al.*, 2005; Jones *et al.*, 2003; Sturm *et al.*, 2005).

The pathophysiological role of 5-oxo-ETE has been difficult to establish, in part due to the lack of an ortholog of the OXE receptor in rodents. Nevertheless, its potent effects on human eosinophils suggest that it might be involved in eosinophilic diseases. In addition to its direct chemoattractant effects on these cells, 5-oxo-ETE has been shown to induce the transendothelial migration of eosinophils (Dallaire *et al.*, 2003). This is due not only to its effect on cell migration, but also to its ability to increase the expression and release of matrix metalloproteinase-9 (MMP-9) as well as the expression of the urokinase-type plasminogen activator receptor (uPAR), resulting in degradation of components of the extracellular matrix, thereby facilitating the passage of eosinophils into the tissues (Guilbert *et al.*, 1999; Langlois *et al.*, 2006). Our prior experiments showing that 5-oxo-ETE can elicit the infiltration of eosinophils into the skin in humans, especially in asthmatic subjects (Muro *et al.*, 2003), would be consistent with a role for this mediator in human inflammatory diseases. We have detected 5-oxo-ETE in feline bronchoalveolar lavage fluid (Cossette *et al.*, 2015) and appreciable levels of this substance have also recently been detected in exhaled breath condensate from humans (Kowal *et al.*, 2017). Furthermore, allergen challenge of house dust mite-sensitive human subjects resulted in significant increases in 5-oxo-ETE, suggesting that it may play a role in asthma (Kowal *et al.*, 2017). Consistent with this, anti-IgE was shown to elicit the release of 5-oxo-ETE from human bronchial segments (Kolmert *et al.*, 2018). 5-Oxo-ETE may also play a role in the development of nasal polyps, as it is formed by

epithelial cells from nasal polyps and was shown to increase the levels of eosinophil cationic protein in organ cultures of nasal polyps (Lin *et al.*, 2018).

Since the potent effects of 5-oxo-ETE are due to its interaction with a selective receptor, rather than to its electrophilic properties (cf. (Schopfer *et al.*, 2011)), a selective OXE receptor antagonist that could block 5-oxo-ETE signaling would be an important asset in determining the pathophysiological role of this lipid mediator and could offer a novel therapeutic approach to alleviate the symptoms of eosinophilic diseases such as asthma, allergic rhinitis and atopic dermatitis. We therefore sought to develop synthetic OXE antagonists with high potency and resistance to metabolism. Using 5-oxo-ETE-induced calcium mobilization in human neutrophils to screen potential antagonists, we identified indoles containing adjacent hexyl and 3*S*-methyl-5-oxovalerate side chains (e.g. ***S*-230**, Fig. 1) as selective OXE antagonists (pIC_{50} ~ 8) (Gore *et al.*, 2014). Because of the absence of the OXE receptor in rodents we looked for an alternative animal model to test the effects of our OXE antagonists in vivo. We first considered cats, which are prone to develop asthma, but, although feline leukocytes respond well to 5-oxo-ETE, our antagonists were not very potent in this species (Cossette *et al.*, 2015), presumably due to differences between the feline and human receptors, which are ~75% identical. We finally settled on cynomolgus monkeys, which have an OXE receptor that is 95% identical to the human receptor. In contrast to its modest effects on feline granulocytes, **230** is a potent inhibitor of 5-oxo-ETE-induced activation of monkey granulocytes (Cossette *et al.*, 2016). High levels of **230** could be detected in the blood shortly after oral administration to monkeys at a dose of 30 mg/kg, but its concentration declined rapidly due to extensive ω-oxidation of the hexyl side chain. In an attempt to reduce ω-oxidation, we replaced the hexyl side chain of ***S*-230** with a phenyl group, resulting in an antagonist (***S*-C025**) that is considerably more potent than ***S*-230** and, despite being cleared fairly rapidly from the blood, displays improved pharmacokinetic properties (Chourey *et al.*, 2018).

Although the monkey is an excellent animal model for investigation of human diseases because of its similarity to humans, the cost of these experiments is very high, and the experimental design is consequently limited due to the relatively small numbers of animals that can be used. Before initiating studies using monkey models of allergic disease, we wished to optimize the properties of the OXE antagonist to be tested in these costly experiments. We therefore sought to optimize our lead compound, ***S*-C025**, with respect to

both potency and pharmacokinetic properties by investigating the effects of a variety of substituents on the phenyl ring. This resulted in the identification of ***S*-Y048**, which has enhanced potency and an increased lifetime in blood, and is converted to an abundant long-lasting plasma metabolite with nearly equivalent potency.

Methods

Ligands and antagonists

5-Oxo-ETE (Khanapure *et al.*, 1998) and LTB_4 (Zamboni & Rokach, 1982) were synthesized as previously described. 5-Oxo-ETE was purified by reversed-phase (RP)-HPLC prior to use. Eotaxin-1 (CCL11) was obtained from Cedarlane, Burlington, Ont, Canada, whereas prostaglandin (PG) D_2 was purchased from Cayman Chemical, Ann Arbor, MI, USA. The procedures for the synthesis of all of the OXE receptor antagonists evaluated in this study have been provided as Supplementary Material.

Measurement of intracellular calcium levels in human neutrophils.

The potencies of OXE receptor antagonists were evaluated by determining their effects on 5-oxo-ETE-induced calcium mobilization in human neutrophils (Gore *et al.*, 2014). Neutrophils were prepared from healthy human subjects after removal of red cells by dextran sedimentation and mononuclear cells by centrifugation over Ficoll-Paque. After labelling the cells with indo-1, fluorescence was measured at 37 °C using a Cary Eclipse spectrofluorometer (Agilent Technologies, Santa Clara, CA) equipped with a temperature-controlled cuvette holder and a magnetic stirrer. After stabilization of the fluorescence, antagonists were added, followed by addition of 5-oxo-ETE (10 nM) 2 min later and digitonin (final concentration 0.1%) after a further 1 min to determine maximal fluorescence.

Measurement of polymerized actin.

F-Actin was measured in unfractionated leukocytes from whole blood obtained from healthy human subjects, following removal of red blood cells using dextran and hypotonic lysis as described previously (Gore *et al.*, 2014), with some minor modifications. The leukocytes were initially incubated with anti-CD16-Pe/Cy5 (1.5 µL/10^6 cells; mouse IgG1, clone 3G8; BioLegend, San Diego, CA; catalogue number 302010; Lot no: B15039; RRID: AB_314210) for 30 min on ice. After centrifugation and washing once with PBS, the cells were suspended in PBS containing Ca^{++} (1.8 mM) and Mg^{++} (1 mM) at a concentration of 5.5×10^6 cells/mL. Aliquots (90 µL) of the labeled cells were preincubated for 5 min at 37 °C with vehicle (1 µL

DMSO) or ***S*-Y048** (10 or 1000 nM), followed by addition of either vehicle (10 μL PBS containing Ca^{++}, Mg^{++}, and 0.1% BSA), 5- oxo-ETE (final concentration, 10 nM), PGD_2 (10 nM), LTB_4 (10 nM) or eotaxin-1 (10 nM). After 20 s, the incubations were terminated by addition of formaldehyde (37%) to give a final concentration of 8.5% and kept on ice for 30 min. A mixture of lysophosphatidylcholine (30 μg in 23.8 μL PBS) and N-(7-nitrobenz-2-oxa-1,3-diazol-4-yl)phallacidin (NBD-phallacidin; Molecular Probes; 49 pmol in 6.2 μL MeOH; final concentration, 0.3 μM) was added to each sample, followed by incubation overnight in the dark at 4 °C. Immediately prior to data acquisition by flow cytometry (BD LSRFortessa X-20, BD Biosciences, San Jose, CA), 300 μL of PBS was added to each sample. Eosinophils were identified by high side scatter and low expression of CD16, whereas neutrophils also displayed high side scatter but high CD16 expression.

Pharmacokinetic experiments in cynomolgus monkeys

Pharmacokinetic experiments were performed using six female cynomolgus monkeys (2.5 to 5 kg), housed at INRS-Institut Armand-Frappier, Laval, Quebec. All experiments were performed in accordance with the guidelines of the Canadian Council on Animal Care as well as the ARRIVE and BJP guidelines and were approved by the local institutional animal care committee. Animals were housed in pairs in cages with a 12 h light/12 h dark schedule. They received a diet consisting of Teklad Global chow for nonhuman primates supplemented with fresh fruit and vegetables and breakfast cereal and had unlimited access to water. Monkeys were first habituated to the oral gavage procedure on three successive days and then weighed to determine the correct dose. Three days later all food was withdrawn at the end of the afternoon and a blood sample was taken. The following morning, various doses of ***S*-Y048**, ***S*-70**, or ***S*-71** were delivered by oral gavage and blood samples (1 ml) were taken from the femoral vein 0.5, 1, 2, 4, 8, 12, and 24 h later. Feeding was resumed after the first blood sample was obtained at 30 min.

To provide a dose of 5 mg kg^{-1}, OXE receptor antagonists (***S*-Y048**, ***S*-70**, and ***S*-71**) were dissolved in ethanol (25 mg mL^{-1}) and stored at -80 °C before use. On the morning of the experiment, the ethanolic solution was thawed and vortexed and the required amount added to 10 volumes of 20 mM $NaHCO_3$ (pH 8.0). The resulting suspension (2.2 mL kg^{-1}; 9.1% EtOH) was immediately vortexed and administered by oral gavage to a monkey. An identical procedure was followed for doses of 2 mg kg^{-1}, except that the antagonist (i.e. ***S*-Y048**) was dissolved in ethanol at a concentration of 10 mg mL^{-1}. In some cases, a second identical dose of antagonist was administered 8 h after the first dose, immediately after obtaining an 8-h

blood sample. Blood samples (1 to 2 mL) were collected in heparinized tubes 1 h prior to gavage and 0.5, 1, 2, 4, 8, 12, and 24 h after gavage. If a second dose was administered, an additional sample was collected 1 h later. The blood samples were centrifuged, and the resulting plasma was frozen and stored at -80 °C prior to extraction and analysis.

Measurement of OXE antagonists and their metabolites in plasma

Plasma samples were thawed and diluted with 2 volumes of MeOH, prior to the addition of internal standards. For analysis of ***S*-Y048**, the tetramethylene analog of C-025 (i.e. 5-(5-chloro-2-(4-phenylbutyl)-1H-indol-3-yl)-3-methyl-5-oxopentanoic acid; 1.3 µg) was used as the internal standard, whereas for ***S*-70** and ***S*-71**, the corresponding pentamethylene analog (i.e. 5-(5-chloro-2-(5-phenylpentyl)-1H-indol-3-yl)-3-methyl-5-oxopentanoic; 1 µg) was used. The samples were stored overnight at -80 °C and the precipitated material was removed by centrifugation. After adjusting the concentration of MeOH in the supernatant to 30% by the addition of water, the sample was loaded onto a C18 Sep-Pak cartridge (Waters Corp), which was washed with 30% MeOH, followed by the elution of the antagonist and its metabolites with 100% MeOH. The solvent was then removed in vacuo using a rotary evaporator, and the residue dissolved in 30% MeOH containing 2.5 mM H_3PO_4 and analyzed by precolumn extraction-RP-HPLC using a modified Waters 2695 Alliance system (Waters Corporation, Mississauga, Ontario, Canada) equipped with a Waters model 2996 photodiode array detector. Automated precolumn extraction was performed as described previously (Powell, 1987) using a C18 SecurityGuard cartridge (4 x 3 mm; Phenomenex, Torrance, CA) coupled with a Kinetex C18 column (Phenomenex; see figure legends for precise chromatographic conditions). All solvents used for extraction and chromatographic analysis were purchased from Fisher Scientific, Markham, ON, Canada.

Normal-phase (NP) HPLC

NP-HPLC of α-hydroxy-**Y048** stereoisomers was performed using an Econosphere column (250 x 4.6 mm; 5 µm particle size; Alltech Associates, Deerfield, IL). The mobile phase was hexane/isopropanol/acetic acid (98.4:1.5:0.1) at a flow rate of 1.5 mL min^{-1} and a temperature of 30 °C.

Chiral HPLC

The *S*- and *R*- enantiomers of compounds **69**-**72** and **Y-048** were separated by chiral HPLC with a Cellulose-1 column (5 µm particle size; 250 x 4.6 mm; Phenomenex) as the stationary phase. Except for compound **70**, isocratic elution was used with a mobile phase consisting of hexane/methanol/acetic acid (98.7:1.2:0.1) with a flow rate of 1.2 mL min^{-1} and a column

temperature of 30 °C. For compound **70**, the mobile phase was hexane/methanol/acetic acid (98.4:1.5:0.1) and the flow rate 1.5 mL min^{-1}.

Stereoisomers of synthetic α-hydroxy-**Y048** as well as ***S*-Y048M** from plasma were analyzed by chiral HPLC using a Cellulose-2 column (4.6 x 250 mm; 5 µm particle size; Phenomenex) with hexane/ethanol/acetic acid (93:7:0.1) as the mobile phase. The flow rate was 1 mL min^{-1} and the column temperature 45 °C.

*Identification of the major plasma metabolite of **S-Y048** by liquid chromatography-tandem mass spectrometry (LC-MS/MS)*

To identify ***S*-Y048M**, column fractions corresponding to the peak at 23.5 min in Fig. 4F were collected during the analysis of a plasma extract from blood obtained 12 h after administration of ***S*-Y048** (5 mg kg^{-1}; see legend to Fig. 5F for further details). The combined fractions were concentrated to dryness in vacuo and dissolved in methanol (100 µL) prior to analysis by LC-MS/MS, which was performed using a model 1100 HPLC system (Agilent Technologies, Santa Clara, CA) connected to an LTQ Velos Orbitrap high resolution mass spectrometer by a heated electrospray ionization source (Thermo Scientific, San Jose, CA). The stationary phase was a Phenomenex Kinetex C18 column (2.6 µm particle size; 50 x 2.1 mm), whereas the mobile phase was a linear gradient between solvents A (0.02% HOAc in water) and B (0.02% HOAc in MeCN) as follows: 0.0 min, 30% B; 1.0 min, 30% B; 25.0 min, 55% B; 32.0 min, 55% B; 32.1 min, 90% B; 37.0 min, 90% B. The flow rate was 0.3 mL min^{-1}, the column temperature 25°C and the injection volume 10 µL. Analyses were performed in negative electrospray ionization (ESI) mode as follows: capillary temperature: 350 °C; source heater temperature: 300 °C; sheath gas flow: 20; auxiliary gas flow: 10; source voltage: - 3.0 kV. The MS settings were: S lens RF level: 60%; automatic gain control (AGC) target: 1 x 10^6 ions; mass range: m/z 250 to m/z 700; resolution: 100,000. Multiple levels of MS^n analysis in data-dependent acquisition (DDA) mode were used to identify ***S*-Y048M**. In DDA mode, the selection of the precursor ion for MS^2 analysis was based on the chlorine isotope pattern and/or isolation of the top three most intense ions from the full MS scan. MS^2 settings were: collision-induced dissociation; signal threshold: 5,000; normalized collision energy: 35; isolation width: 2 Da; activation time: 50 ms. MS^3 was performed using parent and product mass lists to trigger MS^3 for selected ions and was performed with the same settings as MS^2 except that a normalized collision energy of 45 was used.

Data analysis

Data are represented either as individual values or as means ± standard error. The statistical significance of differences among multiple groups was evaluated using one-way ANOVA with the Bonferroni test as a multiple comparison method. Differences between two groups were evaluated using t-tests. Differences with a p value of less than 0.05 were considered to be statistically significant.

Nomenclature of targets and ligands

Key protein targets and ligands in this article are hyperlinked to corresponding entries in http://www.guidetopharmacology.org, the common portal for data from the IUPHAR/BPS Guide to PHARMACOLOGY (Harding *et al.*, 2018), and are permanently archived in the Concise Guide to PHARMACOLOGY 2017/18 (Alexander *et al.*, 2017).

Results

Effects of phenyl ring substituents on OXE antagonist potency

We first examined the abilities of the hydroxyphenyl compounds **74**-**76** to inhibit 5-oxo-ETE-induced calcium mobilization in human neutrophils, but none was as potent as racemic **C025** (pIC_{50}, 9.61 ± 0.07; Fig. 2A). The most potent of these was the p-hydroxy compound **76**, which had a pIC_{50} about 0.3 units lower than that of **C025**, whereas those of the meta and ortho OH-substituted phenyl analogs were about 0.9 and 1.4 units lower (Fig. 2A, 2F). A different pattern emerged when we examined the methoxy-substituted analogs **71**-**73** (Fig. 2B). In this case, the p-methoxy compound (**73**) was the least potent with a pIC_{50} about 0.4 units lower than that of **C025**, whereas the ortho-methoxy compound (**71**) was equipotent and the meta-methoxy compound (**72**) was more potent. A similar pattern was observed for the fluoro-substituted analogs, with the m-fluoro compound (**69**) having a pIC_{50} about 0.5 units higher than **C025** and the ortho and para compounds being less potent (Fig. 2C). However, the most potent among this series of compounds proved to be the m-chloro analog **Y048**, which had a pIC_{50} of 10.47, 0.86 units higher than that of **C025** (Fig. 2D). In contrast, the ortho- and para- chloro compounds **66** and **67** were slightly less potent than **C025**.

*Effect of the length of the methylene chain of **Y048** on antagonist potency*

To examine the effect of the length of the polymethylene chain connecting the m-chlorophenyl group to the indole moiety we prepared the pentamethylene and heptamethylene analogs of **Y048**. Reducing the polymethylene spacer by a single methylene group (compound ***83***) had a large impact on antagonist potency, reducing it by over 50-fold

(Fig. 2E). In contrast, addition of a methylene group, as in the heptamethylene analog ***84***, had relatively little impact on potency.

Potencies of S and R enantiomers of OXE receptor antagonists

All of the data shown in Fig. 2 are for racemic compounds, whereas we have previously shown that most of the antagonist activity of 5-oxo-3-methylvalerate-substituted indoles resides in the *S*-enantiomers (Gore *et al.*, 2014; Reddy *et al.*, 2015). We therefore separated the ***S*** and ***R*** enantiomers of some of the above antagonists by chiral HPLC and examined the potencies of the purified enantiomers. We initially investigated the p-fluoro and o-methoxy compounds, since they were among the first members of this series to be synthesized, and then investigated the more potent meta-substituted compounds. Although the S/R potency ratios differed from one substituent to another, in all cases the *S*-enantiomer was considerably more potent than the corresponding *R*-enantiomer (Table 1). The greatest difference was seen with the methoxy derivatives (ortho and meta), in which case the *S*-enantiomers had pIC_{50} values approximately 2.5 to 3 units higher than the *R*-enantiomers (Table 1 and Fig. 3B, 3C). The difference between enantiomers was less with the fluoro compounds (Fig. 3A, 3D), for which the *S*-enantiomers had pIC_{50} values about 1.1 to 1.7 units higher than the R-enantiomers. Of all the compounds tested, the *S*-enantiomer of the m-chloro compound ***S*-Y048** (pIC_{50},10.81) was the most potent, with the corresponding *R*-enantiomer having a pIC_{50} 1.6 units lower (Fig. 3E).

We also investigated the effects of increasing concentrations of ***S*-Y048** on the concentration-response curve to 5-oxo-ETE (Fig. 3F). Indo-1-loaded neutrophils were preincubated with ***S*-Y048** (20, 200, and 2000 pM) for 2 min prior to the addition of increasing concentrations (2, 20, 200, and 2000 nM) of 5-oxo-ETE and changes in intracellular calcium levels were measured. The lowest concentration of ***S*-Y048** tested (20 pM) resulted in a rightward shift in the concentration-response curve for 5-oxo-ETE and appeared to reduce the maximal response by about 20%. Higher concentrations of ***S*-Y048** further reduced the maximal response to 5-oxo-ETE, which was nearly undetectable at a concentration of 2 nM.

***S*-Y048** *is selective for the OXE receptor*

To ensure that ***S*-Y048** is selective for the OXE receptor we compared its effects to other mediators that activate eosinophils and/or neutrophils. ***S*-Y048** (10 nM) completely blocked actin polymerization induced in human eosinophils by 5-oxo-ETE (10 nM) (Fig. 4A). In contrast, a 100-fold higher concentration of ***S*-Y048** (i.e. 1 µM) had no effect on actin

polymerization in eosinophils in response to identical concentrations of PGD_2, LTB_4 or human eotaxin-1. Similarly, ***S*-Y048** blocked 5-oxo-ETE-induced actin polymerization in neutrophils but had no effect on the response to LTB_4 (Fig. 4B). As expected, neutrophils did not respond to either PGD_2 or eotaxin-1.

In vivo metabolism of OXE receptor antagonists

Because of their much higher potency, we decided to synthesize the *S*-enantiomers of some of the above compounds for further in vivo pharmacokinetic and metabolic studies. We initially prepared the *S*-enantiomers of some of the first compounds that we synthesized for the above in vitro studies, including the p-fluoro compound **70** and the o-methoxy compound **71**. Once we realized the high potency of ***S*-Y048**, purified from racemic **Y048**, we also prepared this compound by total synthesis. Our initial PK experiments were done with the *S*-enantiomers of compounds **70** and **71**. The antagonists were dissolved in ethanol, which was added to bicarbonate, and the resulting suspension was administered by oral gavage at a dose of 5 mg kg^{-1}. Analysis of plasma samples taken 12 h later revealed that, as with the unsubstituted phenyl compound ***S*-C025** (Fig. 5A), substantial levels of ***S*-70** (Fig. 5B) and ***S*-71** (Fig. 5C) were still present. At this time point, for each antagonist we observed a major metabolite with a t_R lower than that of the parent compound. Small amounts of other unidentified metabolites were also present, but we did not observe any other major metabolites with similar or different UV spectra. It is likely that glucuronide conjugates were also formed, but did not reach high concentrations in plasma due to their rapid clearance. We previously detected glucuronides in monkey plasma after administration of the related compound ***S*-230** (Chourey *et al.*, 2017).

The UV spectrum for each of the above major metabolites and their parent compounds are shown in Fig. 5, panels D and E. For each of these metabolites the peak at 303 nm for the parent compound underwent a bathochromic shift to 311 nm, similar to what we previously observed for the major plasma metabolite of ***S*-C025**, which contains a hydroxyl group on the hexamethylene chain on the methylene group adjacent (i.e. alpha) to the indole (Chourey *et al.*, 2018).

We subsequently investigated the in vivo metabolism of the more potent m-chloro antagonist ***S*-Y048**, which was also converted to a major plasma metabolite (***S*-Y048M**; Fig. 5F) with similar UV properties (Fig. 5G). To conclusively identify this metabolite, we isolated it from plasma by RP-HPLC following oral administration of ***S*-Y048** (5 mg/kg) and analyzed it by

LC-MS/MS. ***S*-Y048M** had an $[M-H]^-$ ion at m/z 502.1598, compared to the theoretical value of m/z 502.1557 expected for a hydroxy metabolite of ***S*-Y048** (mass accuracy, 8 ppm). MS^2 fragmentation of this ion (Fig. 5H) resulted in intense ions at m/z 484 (loss of H_2O), 440 (loss of $H_2O + CO_2$), and 292 (base peak, loss of the chlorophenylhydroxyalkyl side chain), consistent with the presence of a hydroxyl group α to the indole. Fragmentation of the ion at m/z 292 gave an MS^3 spectrum (Fig. 5I) with intense ions at m/z 274 (loss of H_2O), 248 (loss of CO_2), 206 (loss of CH_2=CH-CH_2-CO_2H due to a McLafferty rearrangement), and 180. The latter four ions were also observed in the MS^2 spectrum shown in Fig. 5H. We previously observed an intense ion at m/z 292 in the MS^2 spectrum of the α-hydroxy metabolites of ***S*-230** (hexyl group in the 2-position of the indole) (Chourey *et al.*, 2017) and ***S*-C025** (phenylhexyl group in the 2-position of the indole) (Chourey *et al.*, 2018), suggesting that ***S*-C048M** also has a hydroxyl group in this position, and is therefore identical to α-hydroxy-***S*-Y048**.

Pharmacokinetics of OXE receptor antagonists

Fig. 6 shows the plasma levels of the above three compounds as well as ***S*-C025** (Fig. 6A) and their major plasma metabolites over 24 h following oral administration. Preliminary experiments with ***S*-70** (Fig. 6B; n=1) and ***S*-71** (Fig. 6C; n=2) suggest that these compounds have similar PK profiles to that of ***S*-C025** (Table 2). In contrast, ***S*-Y048** appears to have a slightly lower but more prolonged maximal plasma concentration (Fig. 6D). Furthermore, the $t_{½}$ for ***S*-Y048** is about 4 times longer than that for ***S*-C025** ($p < 0.05$) and the area under the curve is about 70% greater ($p < 0.05$) (Table 2). Thus, although the C_{max} for ***S*-Y048** tended to be a little lower than that for ***S*-C025** (not statistically significant), its concentration dropped more slowly over the full 24 h period, at which time the plasma concentration of ***S*-Y048** was about 2.7 times higher than that of ***S*-C025**. However, the latter difference did not quite reach statistical significance, probably due to the limited number of animals (n = 3) that we could study due to the high cost of experiments with monkeys. Another difference between these two antagonists is that the concentrations of the major plasma metabolite of ***S*-C025** (i.e. ***S*-025M**) exceeded those of ***S*-C025** at times longer than 8 h (Fig. 6A), whereas the plasma concentrations of ***S*-Y048** exceeded those of ***S*-Y048M** at 24 h in all three animals in this group (Fig. 6D).

With a single dose of 5 mg kg^{-1}, the plasma levels of ***S*-Y048** were maintained between about 2 and 12 μM over a period of 24 h (Fig. 6D). When a second dose was administered 8 h after the first, the plasma levels of ***S*-Y048** remained between about 5 and 12 μM over 24 h (Fig.

6E). We also examined a lower dose of ***S*-Y048** (2 x 2 mg kg^{-1}, given 8 h apart), which resulted in plasma levels between about 3 and 7 μM over a period of 24 h (Fig. 6F). In a limited number of animals (n = 2) we measured the plasma concentrations of ***S*-Y048** and ***S*-Y048M** over **72** h following administration of ***S*-Y048** at doses of 5 (Fig. 6G) and 2 x 2 (Fig. 6H) mg kg^{-1}. The concentrations of ***S*-Y048M** declined much more slowly than those of its precursor, and between 48 and 72 h were about 2 to 3 times higher with both dosing regimens.

Potencies of major plasma metabolites of OXE receptor antagonists

To determine whether they possess antagonist activity, the metabolites of the o-methoxy, p-fluoro, and m-chloro compounds were purified from plasma by RP-HPLC and their abilities to block 5-oxo-ETE-induced calcium mobilization in neutrophils were compared to those of their parent compounds (Fig. 7, panels A to C). In all cases, the plasma metabolites were potent OXE receptor antagonists, their pIC_{50} values being only about 0.7 units lower than their respective precursors (Table 1). ***S*-Y048M** was the most potent of the metabolites examined, with a pIC_{50} of 10.15.

*Chirality of the α-hydroxyl group in **S*-Y048M***

To determine the chirality of the hydroxyl group alpha to the indole in ***S*-Y048M** and to further investigate the antagonist properties of α-hydroxy-**Y048** stereoisomers, we synthesized a mixture of stereoisomers of this compound, using a procedure similar to that used to prepare the corresponding α-hydroxy derivatives of ***S*-230** (Chourey *et al.*, 2017), and separated them by a combination of normal phase and chiral HPLC. Although we had hoped to synthesize principally the α*S*-OH and α*R*-OH stereoisomers of ***S*-Y048**, in our initial synthesis appreciable amounts of the *R*-methyl stereoisomers were also formed (see Supporting Information for further details), which enabled us to purify all four stereoisomers and examine their antagonist potencies.

Synthetic α-OH-**Y048** was separated into 2 peaks by normal phase-HPLC (Fig. 7D). The material in peak A was then separated into 2 peaks, A_1 (α*R*-OH-***S*-Y048**) and A_2 (α*S*-OH-***R*-Y048**) by chiral HPLC (Fig. 7E). Similarly, the material in peak B was separated into B_1 (α*S*-OH-***S*-Y048**) and B_2 (α*R*-OH-***R*-Y048**) using identical chiral chromatography conditions (Fig. 7F). The above assignments of the chirality of the methyl and hydroxyl groups are based on a combination of chiral synthesis and by analogy between the elution order of α-OH-**Y048** stereoisomers and that of the corresponding stereoisomers of α-OH-**230** (containing a hexyl

side chain instead of a chlorophenylhexyl side chain), which we have characterized using single crystal X-ray diffractometry (Chourey *et al.*, 2017).

The effects of the 4 stereoisomers of α-OH-**Y048** on 5-oxo-ETE-induced calcium mobilization are shown in Fig. 7G. One of the 4 isomers (B_1, α*S*-OH-***S*-Y048**) was extremely potent, with a pIC_{50} approximately equivalent to that of ***S*-Y048**, whereas the other 3 stereoisomers had pIC_{50} values approximately 2 to 3 units lower (Table 3).

A cochromatography experiment was performed to determine the chirality of the α-hydroxyl group in ***S*-Y048M**. ***S*-Y048M** alone gave a single peak when examined by chiral HPLC (Fig. 7H). A chromatogram showing the elution positions of a mixture of synthetic α*S*-OH-***S*-Y048** and α*R*-OH-***R*-Y048** is shown in Fig. 7I, whereas Fig. 7J shows a mixture of these two standards with ***S*-Y048M**. A chromatogram of all 4 of the synthetic stereoisomers, run separately, is also shown in Fig. 7J (dashed lines). ***S*-Y048** is clearly identical to α*S*-OH-***S*-Y048** (Fig. 7K), based both on its antagonist potency and its chromatographic behaviour.

Discussion

The primary objective of the current study was to improve the pharmacokinetic properties and the potency of ***S*-C025** by modification of the phenyl ring. We initially tested the effects of the ortho, meta, and para hydroxy derivatives of **C025**, which we had previously synthesized as potential plasma metabolites of **C025**. However, we were unable to detect significant amounts of any of these compounds in plasma, even with the highest dose (30 mg kg^{-1}) of **C025** tested (data not shown). None of these hydroxy derivatives was as potent as **C025** in blocking the effects of 5-oxo-ETE, with pIC_{50} values between 0.3 and 1.4 units lower than that of the racemic parent compound. Because of their reduced potency and the fact that addition of a hydroxyl group might promote electrophilic substitution of the phenyl ring, which could potentially lead to increased metabolism, we did not investigate the hydroxyphenyl compounds further.

We next examined the antagonist potencies of a series of substituted phenyl compounds containing methoxy, fluoro, and chloro substituents in different position of the phenyl ring. Interestingly, in contrast to the hydroxyphenyl derivatives, among which the p-hydroxy isomer was the most potent, among the halogen and methoxy substituted compounds that we investigated, those with a meta substituent were consistently the most potent, and, in all cases, were more potent than **C025**. This difference could possibly be related to the more

polar nature of the hydroxyl group and its ability to form hydrogen bonds, either with substituents on the receptor or with water molecules.

Of all the compounds we investigated, the m-chloro derivative **Y048** was the most potent. In our previous study, which focused on ***S*-C025**, we examined a series of phenylalkyl compounds containing between 3 and 6 methylene groups and found the hexamethylene analog (i.e. ***S*-C025**) to be the most potent. This also appears to be true for the m-chlorophenyl series, in which case the hexamethylene compound (i.e. ***S*-Y048**) has a pIC_{50} is over 1.7 units higher than the pentamethylene analog **83**. In contrast, addition of another methylene group (heptamethylene compound **84**) did not have an appreciable effect on potency.

To examine the relative potencies of the *R*- and *S*- enantiomers of some of the above compounds, we initially used chiral chromatography to separate the enantiomers from the racemic mixtures. As expected, in all cases the *S*-enantiomers were far more potent than the *R*-enantiomers. We therefore decided to focus on the *S*-enantiomers for further in vivo pharmacokinetic studies, and synthesized several of these compounds by chiral synthesis using a procedure similar to the one we developed for the synthesis of ***S*-230** (Reddy *et al.*, 2015). Because of the far greater quantities of antagonists required for studies in larger animals, as well as the substantial cost of performing in vivo experiments with monkeys, we were able to perform only a limited number of experiments with select compounds. We initially prepared the *S*-enantiomer of the p-fluoro derivative **70**, as the racemic form of this compound was the first in this series to be synthesized. However, because its PK properties did not appear to be substantially different from those of ***S*-C025**, and since it had somewhat reduced potency, we did not pursue this compound further. We next prepared the *S*-enantiomer of another of our early compounds, the o-methoxy derivative **71**, which was approximately equipotent with ***S*-C025** in blocking the OXE receptor, but neither did this compound offer any advantage over ***S*-C025** with respect to its pharmacokinetic properties. The last series of compounds that we synthesized and tested were those containing meta substituents, of which the m-chloro derivative was the most potent, with the racemic compound and the *S*-enantiomer having pIC_{50} values approximately 0.8 units higher than that those of **C025** and its *S*-enantiomer. We therefore prepared ***S*-Y048** by total chemical synthesis and found it to have a much longer half-life in blood as well as a higher area under the curve compared to an equivalent dose of ***S*-C025**. Furthermore, the blood levels of ***S*-**

Y048 could be maintained at a relatively constant level over 24 h by administration of 2 doses 8 h apart.

We previously showed that one of our earlier related antagonists (racemic **230**) selectively blocks 5-oxo-ETE-induced calcium mobilization in neutrophils, without affecting the responses to the neutrophil agonists platelet-activating factor, fMLP and interleukin-8 (Gore *et al.*, 2014). Because our ongoing in vivo studies are focused on eosinophils, we wanted to ensure that ***S*-Y048** is selective for the OXE receptor compared to other receptors involved in the activation of these cells. Taking advantage of flow cytometry to distinguish between eosinophils and neutrophils we found that ***S*-Y048** has no effect on responses of eosinophils mediated by the DP_2, BLT_1, or CCR3 receptors or responses of neutrophils mediated by the BLT_1 receptor.

S*-Y048** is a lipophilic molecule with a calculated Log P (cLogP) value of 5.50, and it is possible that this may contribute to its long lifetime in the blood, as it will be bound to plasma proteins. Although this could theoretically compromise its in vivo efficacy, we have recently shown that this antagonist can block 5-oxo-ETE-induced eosinophil infiltration into the skin of rhesus monkeys and significantly inhibit dermal eosinophilia in response to intradermal injection of house dust mite antigen (Miller *et al.*, 2019). These results clearly demonstrate that the lipophilic nature of ***S*-Y048** does not prevent its in vivo activity in primates, possibly due to its strong binding to the OXE receptor, as it appears to be an insurmountable antagonist, as shown in Fig. 3F. Prolonged receptor residence time due to slow dissociation from a receptor has been shown to be an important determinant of in vivo drug efficacy (Seow *et al.*, 2016). Furthermore, its main plasma metabolite αS-hydroxy-S*-Y048M**) has nearly equivalent potency, a long lifetime in the circulation, and is less lipophilic due to its additional hydroxyl group (cLogP 3.75), and is therefore likely to contribute to the effects of ***S*-Y048**, especially at later time points.

The high potencies of α*S*-hydroxy-***S*-Y048** and the corresponding metabolite of ***S*-C025**, α*S*-hydroxy-***S*-C025**, are very interesting. We identified a similar α*S*-hydroxy metabolite of ***S*-230** (Chourey *et al.*, 2017), but there was a much greater loss of potency (over 2 log units) compared to the corresponding metabolites of the phenyl antagonists. It is clear from our earlier studies that the terminal hydrophobic portion of 5-oxo-ETE is required for its biological activity (Patel *et al.*, 2008), and the addition of a hydrophilic group to this part of the molecule might be expected to interfere with its interaction with the OXE receptor.

However, the presence of a hydroxyl group in the equivalent position of 5-oxo-ETE in the 15-lipoxygenase-generated metabolite 5-oxo-15*S*-HETE, has a relatively modest inhibitory effect on agonist activity (O'Flaherty *et al.*, 1996; Powell *et al.*, 1995; Schwenk & Schröder, 1995), suggesting that a hydroxyl group may be tolerated in this position. The α*R*-hydroxy derivatives of ***S*-Y048**, ***S*-C025**, and ***S*-230** were all far less potent than the metabolically-formed α*S*-hydroxy derivatives. This might possibly be due to differences in the degree of hydrogen bonding between the α-hydroxyl group and the oxo group of the 5-oxovalerate side chain, which could possibly result in a less favorable conformation for the α*R*-hydroxy compounds, thereby impeding their interaction with the OXE receptor.

Because of its potency and prolonged lifetime in the blood, α*S*-hydroxy-***S*-C048** (***S*-C048M**) might in itself be an interesting drug candidate, especially if it is well-absorbed from the GI tract. The slow rate of decline in its plasma concentration over 3 days following administration of ***S*-Y048** suggests that once-daily administration of a relatively low dose might be feasible. However, the two chiral centers of α*S*-hydroxy-***S*-Y048** make its large-scale synthesis more challenging, and we have not yet been able to test this hypothesis.

In conclusion, we have identified a potent OXE receptor antagonist with a pIC_{50} of about 10.8 (~20 pM) in inhibiting calcium mobilization induced by a 500-fold higher concentration of 5-oxo-ETE. ***S*-Y048** appears rapidly in the blood after oral administration, and remains at relatively high levels over 24 h, especially when administered twice daily. In the present study, ***S*-Y048** was administered as a suspension in bicarbonate buffer, but with improved formulation, it should be possible to extend its lifetime in the blood even further. Our initial data from in vivo studies in rhesus monkeys demonstrate that ***S*-Y048** has in vivo efficacy in inhibiting allergen-induced infiltration of eosinophils into the skin (Miller *et al.*, 2019) and lungs (unpublished data). The high potency of ***S*-Y048** together with its favorable PK properties suggest that this OXE receptor antagonist may be a credible drug candidate for the treatment of eosinophilic diseases in humans, such as atopic dermatitis, asthma, and allergic rhinitis.

References

Alexander SPH, Christopoulos A, Davenport AP, Kelly E, Marrion NV, Peters JA, . . . Collaborators C (2017). THE CONCISE GUIDE TO PHARMACOLOGY 2017/18: G protein-coupled receptors. Br J Pharmacol 174**:** S17-S129. https://doi.org/10.1111/bph.13878

Bäck M, Powell WS, Dahlén SE, Drazen JM, Evans JF, Serhan CN, . . . Rovati GE (2014). Update on leukotriene, lipoxin and oxoeicosanoid receptors: IUPHAR Review 7. Brit J Pharmacol 171**:** 3551-3574. https://doi.org/10.1111/bph.12665

Chourey S, Ye Q, Reddy CN, Cossette C, Gravel S, Zeller M, . . . Powell WS (2017). In vivo a-hydroxylation of a 2-alkylindole antagonist of the OXE receptor for the eosinophil chemoattractant 5-oxo-6,8,11,14-eicosatetraenoic acid in monkeys. Biochem Pharmacol 138**:** 107-118. https://doi.org/10.1016/j.bcp.2017.04.031

Chourey S, Ye Q, Reddy CN, Wang R, Cossette C, Gravel S, . . . Powell WS (2018). Novel Highly Potent and Metabolically Resistant Oxoeicosanoid (OXE) Receptor Antagonists That Block the Actions of the Granulocyte Chemoattractant 5-Oxo-6,8,11,14-Eicosatetraenoic Acid (5-oxo-ETE). J Med Chem 61**:** 5934-5948. https://doi.org/10.1021/acs.jmedchem.8b00154

Cossette C, Chourey S, Ye Q, Nagendra Reddy C, Gore V, Gravel S, . . . Powell WS (2016). Pharmacokinetics and metabolism of selective oxoeicosanoid (OXE) receptor antagonists and their effects on 5-oxo-6,8,11,14-eicosatetraenoic acid (5-oxo-ETE)-induced granulocyte activation in monkeys. J Med Chem 59**:** 10127-10146. https://doi.org/10.1021/acs.jmedchem.6b00895

Cossette C, Gravel S, Reddy CN, Gore V, Chourey S, Ye Q, . . . Powell WS (2015). Biosynthesis and actions of 5-oxoeicosatetraenoic acid (5-oxo-ETE) on feline granulocytes. Biochem Pharmacol 96**:** 247-255. https://doi.org/10.1016/j.bcp.2015.05.009

Dallaire MJ, Ferland C, Page N, Lavigne S, Davoine F, & Laviolette M (2003). Endothelial cells modulate eosinophil surface markers and mediator release. Eur Respir J 21**:** 918-924. https://doi.org/10.1183/09031936.03.00102002

Gore V, Gravel S, Cossette C, Patel P, Chourey S, Ye Q, . . . Powell WS (2014). Inhibition of 5-oxo-6,8,11,14-eicosatetraenoic acid-induced activation of neutrophils and eosinophils by novel indole OXE receptor antagonists. J Med Chem 57**:** 364-377. https://doi.org/10.1021/jm401292m

Guilbert M, Ferland C, Bosse M, Flamand N, Lavigne S, & Laviolette M (1999). 5-oxo-6,8,11,14-eicosatetraenoic acid induces important eosinophil transmigration through basement membrane components - Comparison of normal and asthmatic eosinophils. Am J Respir Cell Mol Biol 21**:** 97-104. https://doi.org/10.1165/ajrcmb.21.1.3517

Haeggstrom JZ (2018). Leukotriene biosynthetic enzymes as therapeutic targets. J Clin Invest 128**:** 2680-2690. https://doi.org/10.1172/Jci97945

Harding SD, Sharman JL, Faccenda E, Southan C, Pawson AJ, Ireland S, . . . Nc-Iuphar (2018). The IUPHAR/BPS Guide to PHARMACOLOGY in 2018: updates and expansion to

encompass the new guide to IMMUNOPHARMACOLOGY. Nucleic Acids Res 46: D1091-D1106. https://doi.org/10.1093/nar/gkx1121

Hosoi T, Koguchi Y, Sugikawa E, Chikada A, Ogawa K, Tsuda N, . . . Ohnuki T (2002). Identification of a novel eicosanoid receptor coupled to $G_{i/o}$. J Biol Chem 277: 31459-31465. https://doi.org/10.1074/jbc.M203194200

Iikura M, Suzukawa M, Yamaguchi M, Sekiya T, Komiya A, Yoshimura-Uchiyama C, . . . Hirai K (2005). 5-Lipoxygenase products regulate basophil functions: 5-Oxo-ETE elicits migration, and leukotriene B_4 induces degranulation. J Allergy Clin Immunol 116: 578-585. https://doi.org/10.1016/j.jaci.2005.04.029

Jones CE, Holden S, Tenaillon L, Bhatia U, Seuwen K, Tranter P, . . . Finan P (2003). Expression and characterization of a 5-oxo-6E,8Z,11Z,14Z-eicosatetraenoic acid receptor highly expressed on human eosinophils and neutrophils. Mol Pharmacol 63: 471-477. https://doi.org/10.1124/mol.63.3.471

Khanapure SP, Shi XX, Powell WS, & Rokach J (1998). Total synthesis of a potent proinflammatory 5-oxo-ETE and its 6,7-dihydro biotransformation product. J Org Chem 63: 337-342. https://doi.org/DOI 10.1021/jo9716993

Kolmert J, Fauland A, Fuchs D, Safholm J, Gomez C, Adner M, . . . Wheelock CE (2018). Lipid Mediator Quantification in Isolated Human and Guinea Pig Airways: An Expanded Approach for Respiratory Research. Anal Chem 90: 10239-10248. https://doi.org/10.1021/acs.analchem.8b01651

Kowal K, Gielicz A, & Sanak M (2017). The effect of allergen-induced bronchoconstriction on concentration of 5-oxo-ETE in exhaled breath condensate of house dust mite-allergic patients. Clin Exp Allergy 47: 1253-1262. https://doi.org/10.1111/cea.12990

Langlois A, Ferland C, Tremblay GM, & Laviolette M (2006). Montelukast regulates eosinophil protease activity through a leukotriene-independent mechanism. J Allergy Clin Immunol 118: 113-119. https://doi.org/10.1016/j.jaci.2006.03.010

Lin L, Chen Z, Tang XY, Dai F, Wei JJ, & Sun GB (2018). 5-Oxo-ETE from Nasal Epithelial Cells Upregulates Eosinophil Cation Protein by Eosinophils in Nasal Polyps in vitro. Int Arch Allergy Imm 177: 107-115. https://doi.org/10.1159/000489819

McBrien CN, & Menzies-Gow A (2017). The Biology of Eosinophils and Their Role in Asthma. Front Med (Lausanne) 4: 93. https://doi.org/10.3389/fmed.2017.00093

Miller LA, Cossette C, Chourey S, Ye Q, Reddy CN, Rokach J, & Powell WS (2019). Inhibition of allergen-induced dermal eosinophilia by an oxoeicosanoid (OXE) receptor antagonist in nonhuman primates. Br J Pharmacol In press.

Morita E, Schroder JM, & Christophers E (1989). Differential sensitivities of purified human eosinophils and neutrophils to defined chemotaxins. Scand J Immunol 29**:** 709-716. https://doi.org/10.1111/j.1365-3083.1989.tb01175.x

Muro S, Hamid Q, Olivenstein R, Taha R, Rokach J, & Powell WS (2003). 5-Oxo-6,8,11,14-eicosatetraenoic acid induces the infiltration of granulocytes into human skin. J Allergy Clin Immunol 112**:** 768-774. https://doi.org/10.1067/mai.2003.1736

O'Flaherty JT, Kuroki M, Nixon AB, Wijkander J, Yee E, Lee SL, . . . Daniel LW (1996). 5-Oxo-eicosatetraenoate is a broadly active, eosinophil-selective stimulus for human granulocytes. J Immunol 157**:** 336-342.

Patel P, Cossette C, Anumolu JR, Gravel S, Lesimple A, Mamer OA, . . . Powell WS (2008). Structural requirements for activation of the 5-oxo-6E,8Z, 11Z,14Z-eicosatetraenoic acid (5-oxo-ETE) receptor: identification of a mead acid metabolite with potent agonist activity. J Pharmacol Exp Ther 325**:** 698-707. https://doi.org/10.1124/jpet.107.134908

Peters-Golden M, & Henderson WR, Jr. (2007). Leukotrienes. N Engl J Med 357**:** 1841-1854. https://doi.org/10.1056/NEJMra071371

Powell WS (1987). Precolumn extraction and reversed-phase high-pressure liquid chromatography of prostaglandins and leukotrienes. Anal Biochem 164**:** 117-131. https://doi.org/10.1016/0003-2697(87)90375-7

Powell WS, Chung D, & Gravel S (1995). 5-Oxo-6,8,11,14-Eicosatetraenoic Acid Is a Potent Stimulator of Human Eosinophil Migration. Journal of Immunology 154**:** 4123-4132.

Reddy CN, Ye QJ, Chourey S, Gravel S, Powell WS, & Rokach J (2015). Stereoselective synthesis of two highly potent 5-oxo-ETE receptor antagonists. Tetrahedron Lett 56**:** 6896-6899. https://doi.org/10.1016/j.tetlet.2015.10.097

Schopfer FJ, Cipollina C, & Freeman BA (2011). Formation and Signaling Actions of Electrophilic Lipids. Chemical Reviews 111**:** 5997-6021. https://doi.org/10.1021/cr200131e

Schwenk U, & Schröder JM (1995). 5-Oxo-eicosanoids are potent eosinophil chemotactic factors - functional characterization and structural requirements. J Biol Chem 270**:** 15029-15036.

Seow V, Lim J, Cotterell AJ, Yau MK, Xu W, Lohman RJ, . . . Fairlie DP (2016). Receptor residence time trumps drug-likeness and oral bioavailability in determining efficacy of complement C5a antagonists. Sci Rep-Uk 6**:** 24575. https://doi.org/10.1038/srep24575

Sturm GJ, Schuligoi R, Sturm EM, Royer JF, Lang-Loidolt D, Stammberger H, . . . Heinemann A (2005). 5-oxo-6,8,11,14-eicosatetraenoic acid is a potent chemoattractant for human basophils. J Allergy Clin Immunol 116**:** 1014-1019. https://doi.org/10.1016/j.jaci.2005.08.001

Sun FF, Crittenden NJ, Czuk CI, Taylor BM, Stout BK, & Johnson HG (1991). Biochemical and Functional Differences between Eosinophils from Animal Species and Man. J Leukocyte Biol 50**:** 140-150.

Takeda S, Yamamoto A, & Haga T (2002). Identification of a G protein-coupled receptor for 5-oxo-eicosatetraenoic acid. Biomedical Research-Tokyo 23**:** 101-108. https://doi.org/10.2220/biomedres.23.101

Yokomizo T, Nakamura M, & Shimizu T (2018). Leukotriene receptors as potential therapeutic targets. J Clin Invest 128**:** 2691-2701. https://doi.org/10.1172/JCI97946

Zamboni R, & Rokach J (1982). Simple Efficient Synthesis of Ltb4 and 12-Epi-Ltb4. Tetrahedron Lett 23**:** 2631-2634. https://doi.org/Doi 10.1016/S0040-4039(00)87415-8

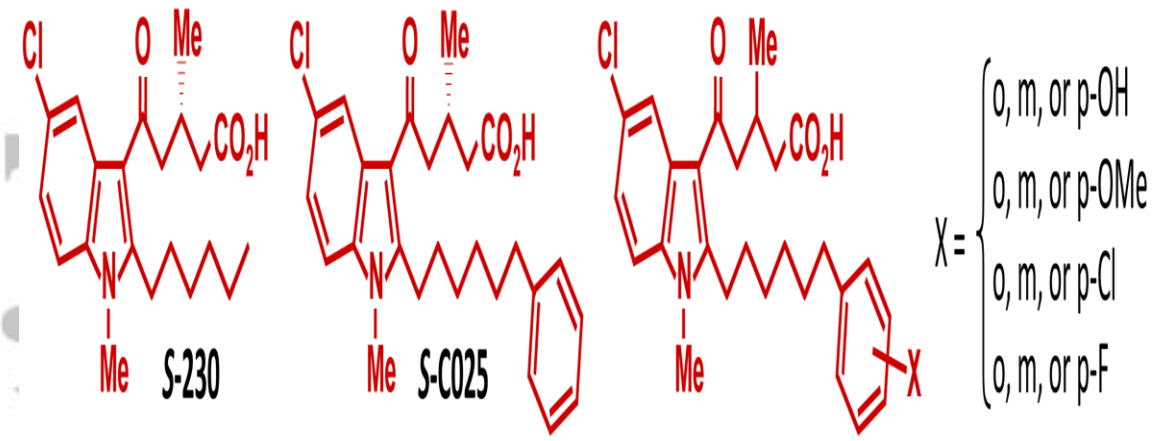

Figure 1. Structures of OXE receptor antagonists.

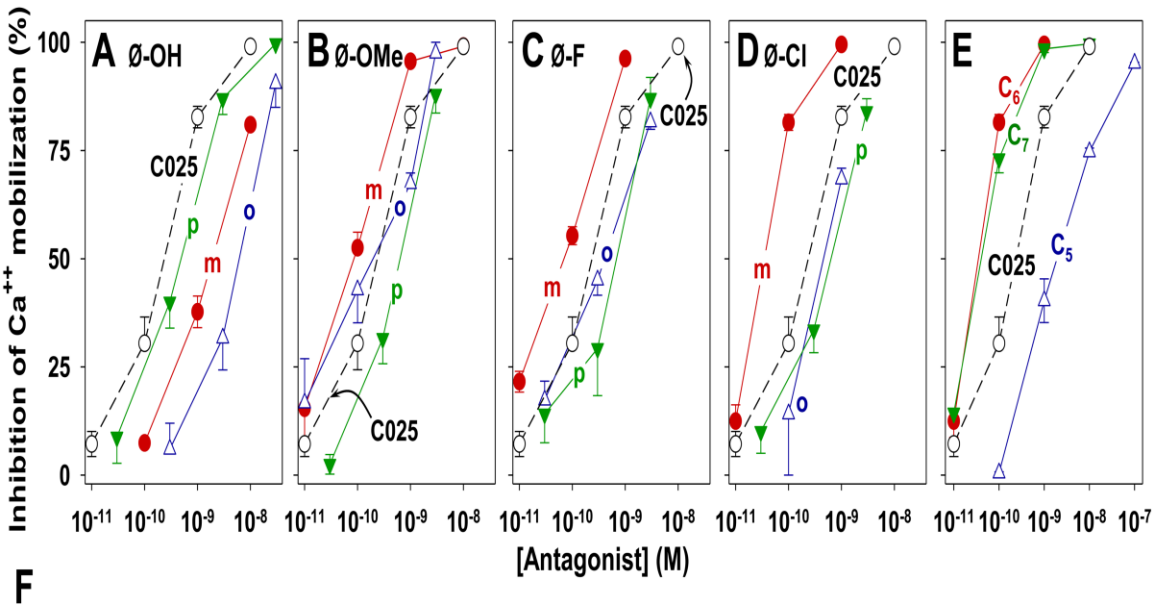

F

pIC_{50} values for inhibition of 5-oxo-ETE-induced calcium mobilization

Substituent (X)	n	Cpd #	Ortho (Δ)	Cpd #	Meta (●)	Cpd #	Para (▼)
OH	6	***74***	8.20 ± 0.10 (2)	***75***	8.73 ± 0.06 (3)	**76**	9.33 ± 0.10 (6)
OMe	6	***71***	9.64 ± 0.12 (5)	***72***	10.11 ± 0.10 (6)	**73**	9.21 ± 0.05 (5)
F	6	***68***	9.43 ± 0.08 (6)	***69***	10.15 ± 0.04 (3)	**70**	9.27 ± 0.21 (6)
Cl	6	***66***	9.42 ± 0.17 (3)	***Y048***	**10.47 ± 0.03 (9)**	**67**	9.25 ± 0.16 (3)
Cl	5			***83***	8.74 ± 0.10 (3)		
Cl	7			***84***	10.23 ± 0.09 (3)		

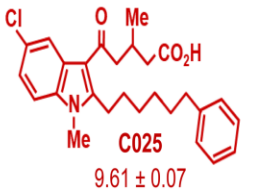

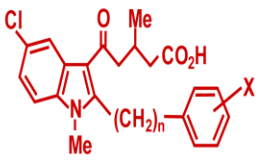

Figure 2. Effects of ortho- meta- and para- substituents on antagonist potency. The effects of analogs of racemic ***025*** containing hydroxyl (**A**), methoxyl (**B**), fluoro (**C**), and chloro (**D**) substituents in the ortho (o; Δ), meta (m; ●), and para (p; ▼) positions on 5-oxo-ETE-induced calcium mobilization were determined. **E**: Effect of the length of the polymethylene spacer (C_5, Δ; C_6 (i.e. Y048), ●; C_7, ▼) on the potency of m-Cl-substituted antagonists. **E**: Table showing the pIC_{50} values for all of the compounds depicted in panels A to E. The values are means ± SE with the numbers of independent experiments indicated in brackets. All compounds are racemic mixtures. Data for **C025** (○; pIC_{50}, 9.61 ± 0.07 (n = 10)), which was included in this experiment for comparison, are also shown.

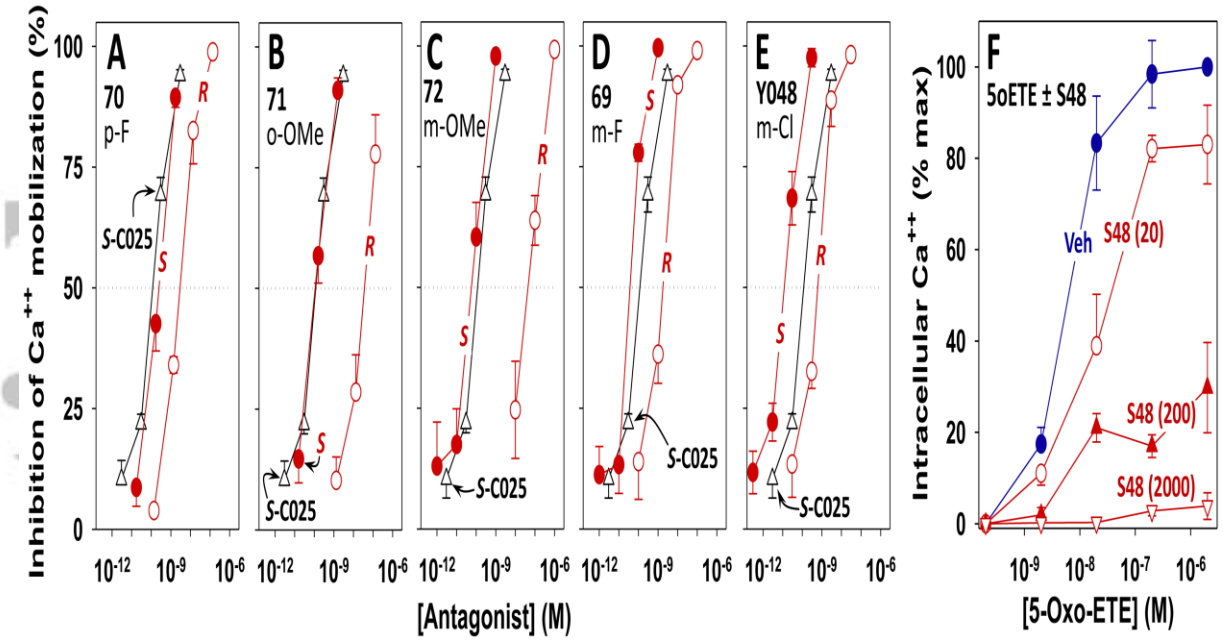

Figure 3. Effects of the S and R enantiomers of OXE-R antagonists on 5-oxo-ETE-induced calcium mobilization. The effects of the S (●) and R (○) enantiomers of **A**: p-fluoro (**70**), **B**: o-methoxy (**71**), **C**: m-methoxy (**72**), **D**: m-fluoro (**69**), and **E**: m-chloro (**Y048**) substituted phenyl antagonists on calcium mobilization induced in human neutrophils by 10 nM 5-oxo-ETE are shown. The response to ***S*-C025** (Δ; pIC_{50}, 10.06 ± 0.01) is included for comparison. The values are means ± SE (See Table 1 for numbers of experiments). **F**: Effects of increasing concentrations of ***S*-Y048** (S48) on the concentration-response curve for 5-oxo-ETE-induced calcium mobilization in human neutrophils. Either vehicle (●) or different concentrations (20 pM, o; 200 pM, ▲, or 2000 pM, ∇) of ***S*-Y048** were added to indo-1-loaded neutrophils, followed 2 min later by the addition of different concentrations of 5-oxo-ETE, (see Methods section for further details).

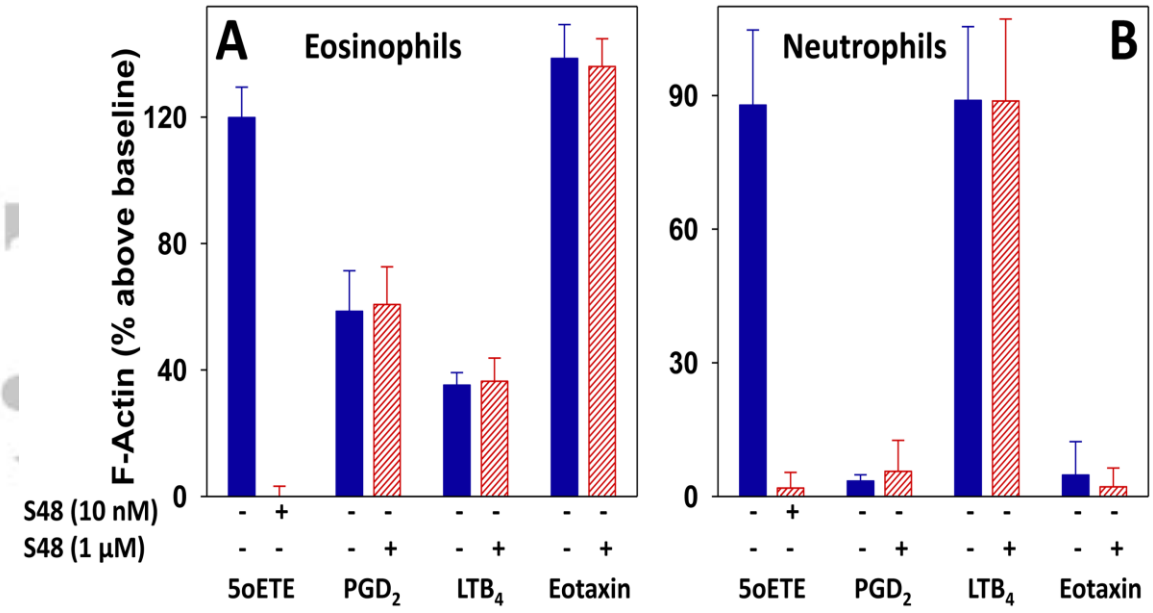

Figure 4. Selectivity of *S*-Y048 for the OXE receptor. Unfractionated human leukocytes labeled with anti-CD16-PE/Cy5 were incubated for 5 min with either vehicle or concentrations of ***S*-Y048** (S48) of either 10 nM (5-oxo-ETE) or 1 µM (all other agonists). 5-Oxo-ETE, PGD_2, LTB_4, or eotaxin-1 (all 10 nM) were then added and incubations were terminated after a further 20 s by the addition of formaldehyde. Polymerized F-actin was measured in eosinophils and neutrophils by flow cytometry as described in the Methods section.***S*-C025** (**F, G**), all at doses of 5 mg/kg, were administered to monkeys by oral gavage and blood samples (1 ml) were taken after 12 h. Internal standards (tetramethylene analog of **C025** for ***S*-C025** and ***S*-Y048** and pentamethylene analog of **C025** for compounds ***S*-70** and ***S*-71**) were added to the plasma samples, which were extracted and analyzed by RP-HPLC. For ***S*-C025** (panel **A**), the data was taken from a previous study (Chourey *et al.*, 2018) employing a Novapak C18 column and a gradient of 70 to 100% MeCN over 15 min. For panels **B** and **C** a Kinetex C18 column (2.6 µm particle size; 100 x 4.6 mm) was used with a gradient between 38 and 65% MeCN over 35 min, followed by 5 min at 65% MeCN. For panel **F**, a Kinetex C18 column (5 µm particle size; 250 x 4.6 mm) was used with a gradient between 55 and 75% MeCN over 30 min, followed by 5 min at 75% MeCN. All solvents contained 0.02% HOAc. The flow rates were 1 ml/min and the column temperature was maintained at 30 °C. The UV spectra of ***S*-70**, ***S*-71**, and ***S*-Y048** (broken lines) along with their major plasma metabolites (red solid lines) are shown in panels **D**, **E**, and **G**, respectively. **H**: MS^2 fragmentation of the $[M-H]^-$ ion at m/z 502 for ***S*-Y048M**, isolated from plasma as shown in panel **F**. **I**: MS^3 fragmentation of the ion at m/z 292 shown in panel **H**. The ion at m/z 206 is formed as the result of a McLafferty rearrangement.

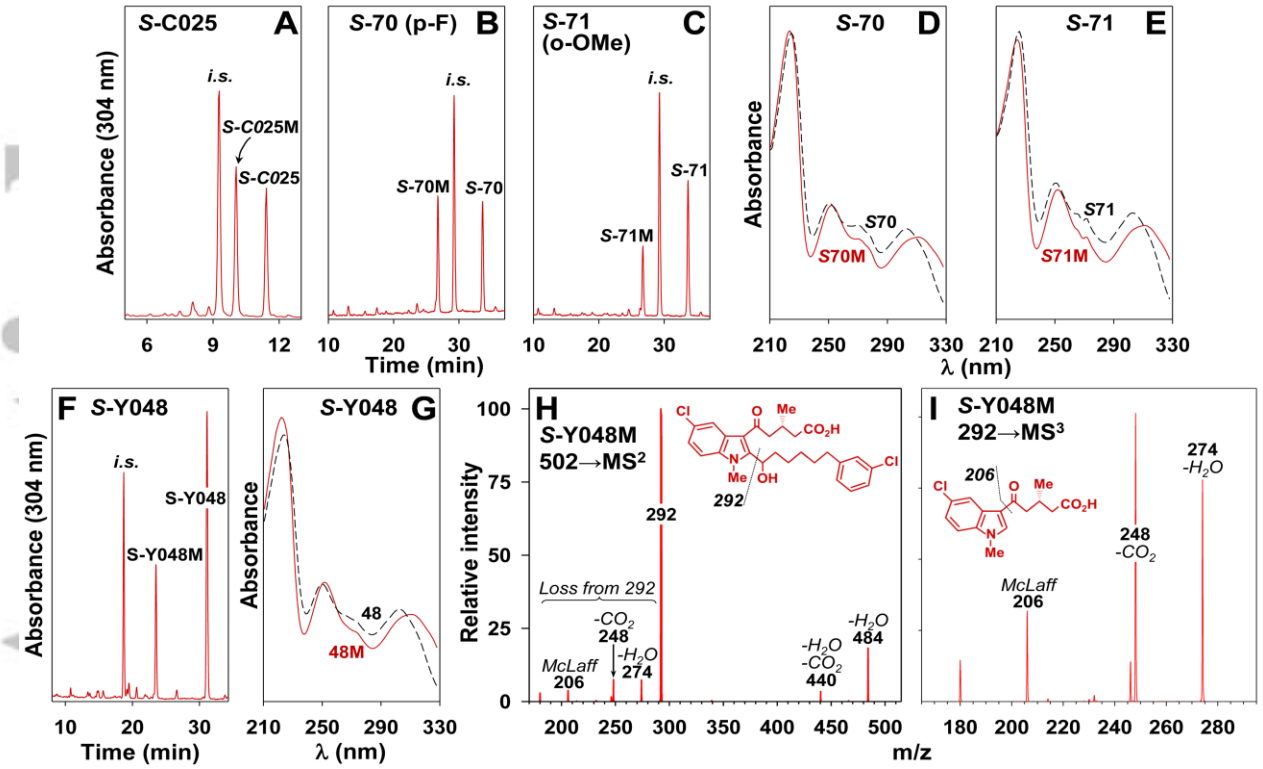

Figure 5. Identification of major plasma metabolites of OXE receptor antagonists. *S*-C025 (A), *S*-70 (p-fluoro-***S*-C025**) **(B, D)**, ***S*-71** ((o-methoxy-***S*-C025**) **(C, E)**, and ***S*-Y048** (m-chloro-***S*-C025** **(F, G)**, all at doses of 5 mg/kg, were administered to monkeys by oral gavage and blood samples (1 ml) were taken after 12 h. Internal standards (tetramethylene analog of **C025** for ***S*-C025** and ***S*-Y048** and pentamethylene analog of **C025** for compounds ***S*-70** and ***S*-71**) were added to the plasma samples, which were extracted and analyzed by RP-HPLC. For ***S*-C025** (panel **A**), the data was taken from a previous study (Chourey *et al.*, 2018) employing a Novapak C18 column and a gradient of 70 to 100% MeCN over 15 min. For panels **B** and **C** a Kinetex C18 column (2.6 µm particle size; 100 x 4.6 mm) was used with a gradient between 38 and 65% MeCN over 35 min, followed by 5 min at 65% MeCN. For panel **F**, a Kinetex C18 column (5 µm particle size; 250 x 4.6 mm) was used with a gradient between 55 and 75% MeCN over 30 min, followed by 5 min at 75% MeCN. All solvents contained 0.02% HOAc. The flow rates were 1 ml/min and the column temperature was maintained at 30 ºC. The UV spectra of ***S*-70**, ***S*-71**, and ***S*-Y048** (broken lines) along with their major plasma metabolites (red solid lines) are shown in panels **D**, **E**, and **G**, respectively. **H**: MS^2 fragmentation of the $[M - H]^-$ ion at m/z 502 for ***S*-Y048M**, isolated from plasma as shown in panel **F**. **I**: MS^3 fragmentation of the ion at m/z 292 shown in panel **H**. The ion at m/z 206 is formed as the result of a McLafferty rearrangement.

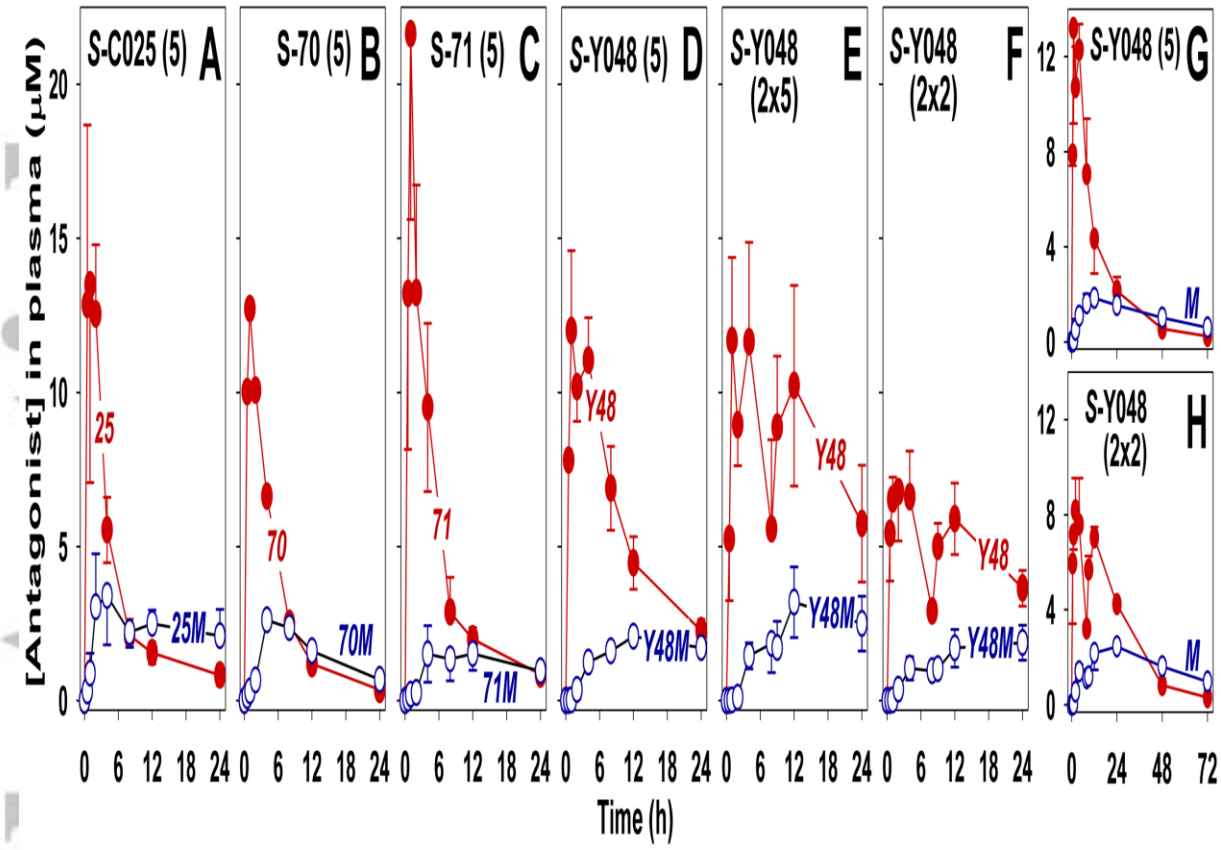

Figure 6. Levels of OXE receptor antagonists and their major metabolites in plasma following oral administration. OXE receptor antagonists were administered to cynomolgus monkeys by oral gavage as described in Methods. Blood samples were collected after various times and the plasma was subjected to solid-phase extraction and the amounts of unmetabolized antagonist (●) along with their major plasma metabolite (○) were measured by RP-HPLC, using appropriate internal standards as shown in Fig. 5. Data for ***S*-C025** (5 mg/kg; n = 3), taken from a previous study (Chourey *et al.*, 2018), are shown in panel **A**. **B**: ***S*-70** (p-fluoro; 5 mg/kg; n = 1); **C**: ***S*-71** (o-methoxy; 5 mg/kg; n = 2); **D**: ***S*-Y048** (m-chloro; 5 mg/kg; n = 3); **E**: ***S*-Y048** (5 mg/kg followed 8 h later by a second dose of 5 mg/kg); **F**: ***S*-Y048** (2 mg/kg followed 8 h later by a second dose of 2 mg/kg). In two animals, measurements of ***S*-Y048** and ***S*-Y048M** (M) were made up to 72 h for doses of ***S*-Y048** of 5 mg/kg (**G**) and 2 x 2 mg/kg (**H**).

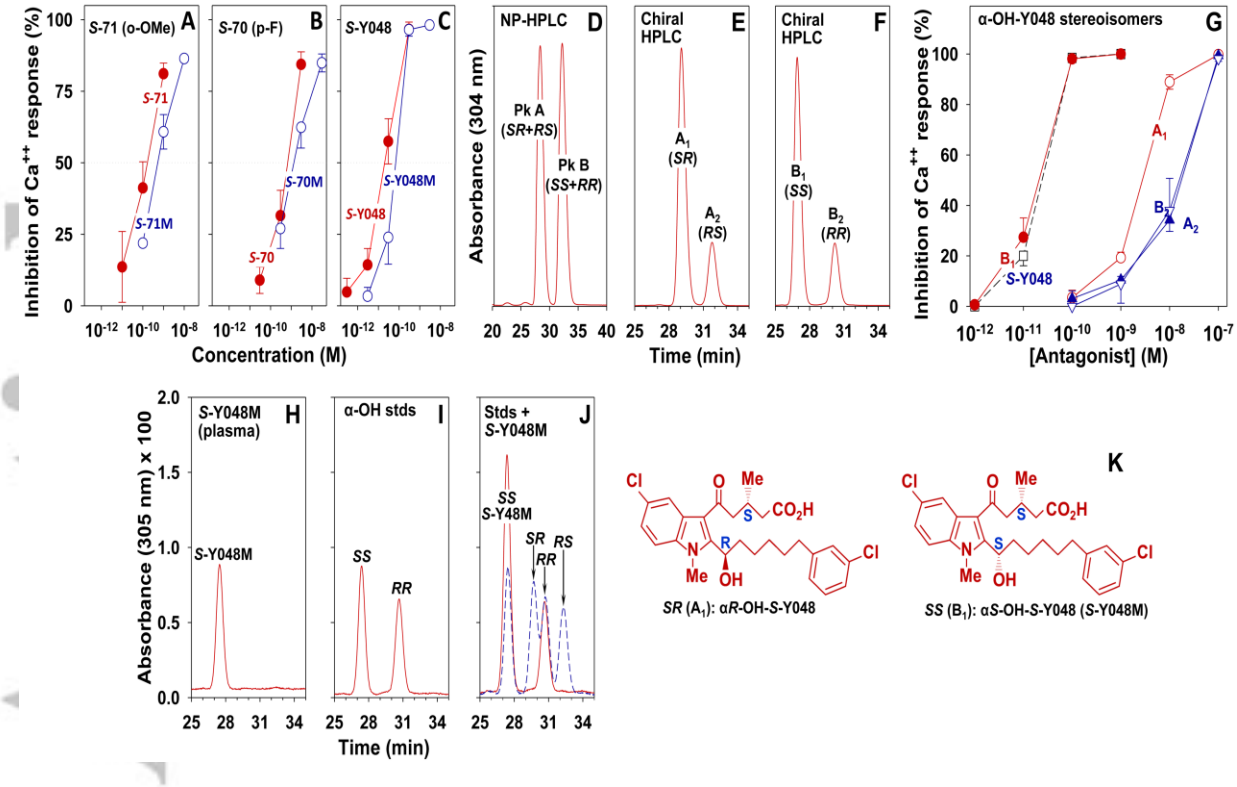

Figure 7. Antagonist potencies of the major plasma metabolites and their synthetic stereoisomers of some OXE receptor antagonists. The major plasma metabolites of ***S*-71** (o-methoxy-***S*-C025**) (**A**), ***S*-70** (p-fluoro-***S*-C025)** (**B**), and ***S*-Y048** (m-chloro-***S*-C025**) (**C**) weremobilization in neutrophils. The values for antagonists (●) and their metabolites (○) are means ± SE (n = 3), except for the data shown in panel C (n = 6). **Panels D-F:** α*RS*-Hydroxy-***RS*-Y048** was prepared using the chiral synthon methyl (*R*)-5-chloro-3-methyl-5-oxopentanoate (*R*:*S* = 9:1), which in this preparation resulted in mixture of stereoisomers of α-OH-**Y048** in which the S:R ratio for the methyl group in the acyl side chain of the final product was about 4:1. **D**: Separation of *RR*/*SS* enantiomer pair from *RS*/*SR* enantiomer pair by NP-HPLC. **E**: Separation of the *SR* and *RS* enantiomers from Peak A in panel **D** by chiral HPLC. **F**: Separation of the *SS* and *RR* enantiomers from Peak B in panel **D** by chiral HPLC. **G**: Effects of synthetic ***S*-Y048** (□), A_1 (○; α*R*-hydroxy-***S*-Y048**), A_2 (▲; α*S*-hydroxy-***R*-Y048**), B_1 (●, α*S*-hydroxy-***S*-Y048**), and B_2 (▽; α*R*-hydroxy-***R*-Y048**) on 5-oxo-ETE-induced calcium mobilization in human neutrophils. **H**: Chiral HPLC of ***S*-Y048M** after isolation from plasma by RP-HPLC. **I**: Chiral HPLC of a mixture of synthetic α*S*-OH-***S*-Y048** and α*R*-OH-*R*-**Y048**; **J**: Cochromatography of ***S*-Y048M** with the standards shown in panel **I**. The dashed blue curve shows a mixture of all 4 synthetic stereoisomers, run separately. **K**: Structures of α*S*-hydroxy-***S*-Y048** (*SS*) and α*R*-hydroxy-***S*-Y048** (*SR*). See the Methods section for the NP and chiral HPLC conditions.